Carbohydrate Polymers 344 (2024) 122518

Contents lists available at ScienceDirect

Carbohydrate Polymers

journal homepage: www.elsevier.com/locate/carbpol

Phosphorylation-dependent immunomodulatory properties of B.PAT polysaccharide isolated from *Bifidobacterium animalis* ssp. *animalis* CCDM 218

Katarzyna Pacyga-Prus [a,*], Corine Sandström [b], Dagmar Šrůtková [c], Martin Schwarzer [c], Sabina Górska [a,*]

[a] Laboratory of Microbiome Immunobiology, Hirszfeld Institute of Immunology and Experimental Therapy, Polish Academy of Sciences, 53-114 Wroclaw, Poland
[b] Department of Molecular Sciences, Swedish University of Agricultural Sciences, Box 7015, SE-750 07 Uppsala, Sweden
[c] Laboratory of Gnotobiology, Institute of Microbiology, Czech Academy of Sciences, 549 22 Novy Hradek, Czech Republic

ARTICLE INFO

Keywords:
Polysaccharides
Bifidobacterium
Dephosphorylation
Immunomodulation
Surface antigens
Postbiotics

ABSTRACT

A wide range of articles describe the role of different probiotics in the prevention or treatment of various diseases. However, currently, the focus is shifting from whole microorganisms to their easier-to-define components that can confer similar or stronger benefits on the host. Here, we aimed to describe polysaccharide B.PAT, which is a surface antigen isolated from *Bifidobacterium animalis* ssp. *animalis* CCDM 218 and to understand the relationship between its structure and function. For this reason, we determined its glycerol phosphate-substituted structure, which consists of glucose, galactose, and rhamnose residues creating the following repeating unit:

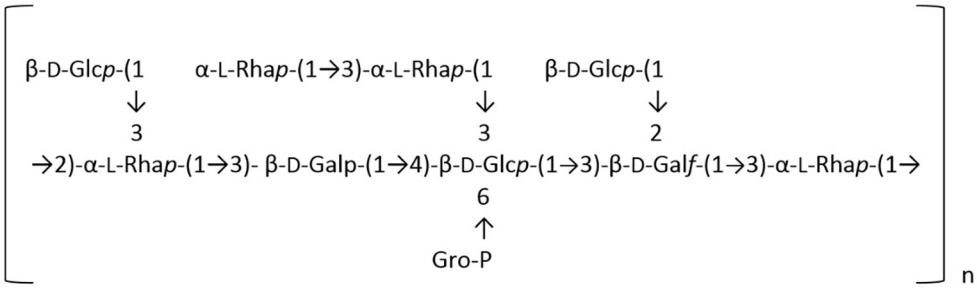

To fully understand the role of glycerol phosphate substitution on the B.PAT function, we prepared the dephosphorylated counterpart (B.MAT) and tested their immunomodulatory properties. The results showed that the loss of glycerol phosphate increased the production of IL-6, IL-10, IL-12, and TNF-α in bone marrow dendritic cells alone and after treatment with *Lacticaseibacillus rhamnosus* GG. Further studies indicated that dephosphorylation can enhance B.PAT properties to suppress IL-1β-induced inflammatory response in Caco-2 and HT-29 cells. Thus, we suggest that further investigation of B.PAT and B.MAT may reveal distinct functionalities that can be exploited in the treatment of various diseases and may constitute an alternative to probiotics.

1. Introduction

The microbiome composition and function have recently gained immense attention, and the number of publications on this topic started to grow extensively after 2010. Currently, not only living and proliferating bacteria (called probiotics) but also their isolated and defined

* Corresponding authors.
E-mail addresses: katarzyna.pacyga-prus@hirszfeld.pl (K. Pacyga-Prus), corine.sandstrom@slu.se (C. Sandström), sabina.gorska@hirszfeld.pl (S. Górska).

https://doi.org/10.1016/j.carbpol.2024.122518
Received 18 March 2024; Received in revised form 15 July 2024; Accepted 17 July 2024
Available online 18 July 2024

components are considered health-promoting factors (Salminen et al., 2021). These molecules are referred to as postbiotics and include surface antigens, for instance, lipoteichoic acids, proteins, glycolipids, and polysaccharides (PSs) (Pyclik et al., 2020). The last group is well described in the literature for both gram-positive and gram-negative bacteria. PSs can be a part of the O-antigen in lipopolysaccharides (LPS, in gram-negative bacteria), can be present in an unattached form in slime, or can be anchored to a cell surface (Bazaka et al., 2011). In general, PSs are composed of monosaccharides connected by glycosidic bonds, creating units that may be modified by different substitutions (Zeidan et al., 2017).

Polysaccharides of microbial origin are widely applied in medicine and industry. Some, like hyaluronic acid produced by bacteria (such as *Streptococci*), are extensively used *e.g.* in cosmetology (Bravo et al., 2022). Others, like dextran (produced by lactic acid bacteria), due to their high viscosity and emulsifying and stabilizing properties, have been tested as potential candidates for modern drug delivery systems (Hu et al., 2021). Additionally, the direct and indirect influence of polysaccharides on apoptotic cell death, antimetastasis, or immunomodulation has been described in the literature (Prateeksha et al., 2022). For instance, the polysaccharide Maitake Z produced by *G. frondosa* improves the Th1-related response against tumor development by upregulating the cytokines IL-12, IL-2, and IFN-γ (Masuda et al., 2009). The immunomodulatory functions of the extracellular PSs of health-promoting bacteria have been extensively described in the literature (Pacyga-Prus et al., 2023; Schiavi et al., 2018; Speciale et al., 2019; Srutkova et al., 2023; Verma et al., 2018). Primarily, their role was directly related to the protection, support, and energy supply for microorganisms. However, more publications have described their host-related functions (Khan et al., 2022). The ability of PSs to influence immune system function by activating different cell subsets or by inducing anti-inflammatory, pro-inflammatory, or regulatory cytokines and chemokines is particularly interesting (Górska et al., 2014; Nishimura-Uemura et al., 2003; Pacyga-Prus et al., 2023; Sato et al., 2004; Speciale et al., 2019; Verma et al., 2018). These functions may be crucial for the prevention or treatment of a wide variety of diseases. For instance, Yue et al. described EPS-1, EPS-2, and EPS-3 PSs from *Bifidobacterium longum* subsp. *infantis* E4 and their role in the inhibition of the pro-inflammatory factors' expression while inducing anti-inflammatory TGF-β and IL-10. These results indicated their role in the alleviation of inflammation. Moreover, they were able to increase the proliferation of mouse spleen lymphocytes and promote NK cell activity (You et al., 2020). On the other hand, BAP1 PS from *Bifidobacterium adolescentis* CCDM 368 exhibited a potential role in allergy treatment by strong induction of IFN-γ and inhibition of Th2-related cytokines in cells isolated from OVA-sensitized mice. More importantly, it was efficiently transferred from epithelial to dendritic cells (Pacyga-Prus et al., 2023).

Depending on their origin, monosaccharide composition, size, spatial structure, or substitutions, PSs can exhibit a wide range of properties, including anti-oxidative, anti-tumor, or anti-microbial functions (Angelin & Kavitha, 2020). These substitutions include, among others, acetylation, sulfation, or phosphorylation. The presence of chemical modifications may influence the charge, molecular weight, or spatial structure of PSs and thus have a great impact on their function and biological activities. In a great number of examples, substitutions can solve the problem of poor solubility or low bioactivity of PSs (Cao et al., 2020; Liu et al., 2023). However, the natural occurrence of chemically modified PSs is low, as is the degree of substitution of the PS chain. For this reason, to improve PSs' functions, non-substituted PSs are modified in the research and industry fields to obtain new PSs that acquire enhanced functionalities (Laffargue et al., 2023). Among bacteria, there are naturally occurring PSs that bear phosphorylation in their structure, however, only a few publications have investigated the influence of this substitution on PSs function (Nishimura-Uemura et al., 2003; Sato et al., 2004; Speciale et al., 2019). Moreover, there is little information on the structure-function relationships. This can be caused by the complex, hard-to-characterize backbones that make the structure very difficult to determine (Laffargue et al., 2023).

The beneficial effects of probiotics in inflammatory disorders (such as inflammatory bowel disease or allergy) are well described in the literature, however, their use is not without drawbacks. Researchers are therefore focusing on finding alternative molecules that will inherit the immunomodulatory effect of whole microorganisms and overcome emerging obstacles. One solution focuses on the use of postbiotics that have decisive advantages over whole microorganisms. First, polysaccharides are inanimate molecules that cannot reproduce and thus cause bacteremia (Salminen et al., 2021). Second, their structure is much easier to define, which allows a detailed examination of their safety and exact functions. Moreover, PSs are stable molecules that are heat resistant and can be stored at room temperature (RT), which makes them easier to transport than probiotics (Rafique et al., 2023). Although microbial PSs have gained increased amounts of attention over the past decade, there are no known available probiotic alternatives. However, immunomodulatory results are promising for quick changes.

Here, we propose that the presence of phosphate substitution impacts the immunomodulatory function of PSs isolated from *Bifidobacterium animalis* ssp. *animalis* CCDM 218 (Ba218). Therefore, in this study, a PS called B.PAT was isolated from the surface of the Ba218 strain. Its structure was described with the use of NMR and GLC-MS methods, and the presence of glycerol phosphate substitution was confirmed by ^{31}P NMR and ^{1}H—^{13}C HSQC experiments. To fully understand the role of phosphorus substitution, B.PAT was dephosphorylated with the use of 48 % hydrofluoric acid. The differences in the immunomodulatory properties between B.PAT (phosphorylated PS) and B.MAT (dephosphorylated PS) were tested on bone marrow-derived dendritic cells (BMDCs) from BALB/c mice. Finally, to investigate the potential anti-inflammatory functions, both PSs were studied in the Caco-2/HT-29 cell line model of IL-1β-induced inflammation. As expected, B.PAT and B.MAT exhibited distinct properties depending on the presence of the phosphate substitution.

2. Materials and methods

2.1. *Bifidobacterium animalis ssp. animalis CCDM 218 culture*

Ba218, originally isolated from a healthy human fecal sample (Srutkova et al., 2015), was obtained from the Czech Collection of Dairy Microorganisms (CCDM, Laktoflora, Milcom, Tábor, Czech Republic). Bacteria were cultivated on MRS broth (Sigma Aldrich) supplemented with 0.05 % L-cysteine (Merc Millipore) for 72 h at 37 °C under anaerobic conditions (anaerobic chamber, Oxoid, 80 % N_2, 10 % CO_2, 10 % H_2). For bacterial mass collection, Ba218 was centrifuged at 4500 ×*g* (15 min, 4 °C; Hermle Centrifuge Z 36 HK) and washed twice with sterile phosphate-buffered saline (PBS), after which the resulting pellet was frozen and freeze-dried.

2.2. *Polysaccharide isolation and purification*

The Ba218 PSs were isolated as described previously according to the method commonly used in our laboratory (Pacyga-Prus et al., 2023). Briefly, the crude PS mixture was extracted by bacterial incubation in 10 % trichloroacetic acid (2.5 h, RT) and centrifugation (15,000 ×*g*, 4 °C, 20 min; Hermle Centrifuge Z 36 HK). For higher efficiency, the extraction was repeated twice. The collected supernatant was treated with 5 volumes of ethanol and kept overnight at −20 °C. Then, the suspension was centrifuged (15,000 ×*g*, 4 °C, 50 min, Hermle Centrifuge Z 36 HK), dissolved and dialyzed with miliQ water (24 h, 4 °C) (MWCO 6–8 kDa, Roth). The obtained crude mixture was frozen, freeze-dried, and subsequently subjected to ion exchange (DEAE-Sephadex A-25 column; 1.6 × 20 cm (Pharmacia); buffer A: 20 mM Tris-HCl, buffer B: 2 M NaCl; linear-gradient (0 % B – 100 % B); 23 °C) and size exclusion (TSK HQ-55S column; 1.6 × 100 cm (Amersham Pharmacia Biotech);

eluted with 0.1 M ammonium acetate; 23 °C) chromatography with the use of the NGS Chromatography System (Bio-Rad) equipped with a UV detector. To detect sugars, the fractions collected after separations were tested with the phenol-sulfuric acid method (DuBois et al., 1956). Finally, the PS fractions were analyzed using classical chemical methods and NMR spectroscopy.

To obtain a dephosphorylated fraction, 5 mg of B.PAT PS was treated with 48 % hydrofluoric acid for 48 h at 4 °C. Afterward, the dephosphorylated sample (B.MAT) was dialyzed overnight with miliQ water using Slide-A-Lyzer™ Dialysis Cassettes (2 K MWCO, Thermo Scientific). The efficiency of dephosphorylation was assessed by ^{31}P NMR and ^{1}H—^{31}P HSQC NMR experiments.

The average molecular mass of the PS was determined as described previously by GPC (Dionex Ultimate 3000) on an OHpak SB-806 M HQ column (8 × 300 mm, maximum pore size 15,000 Å; Shodex) equipped with a refractive index detector (RI 102; Shodex). Briefly, dextran standards (MW 12, 25, 50, 80, 150, and 270 kDa) were administered on a column together with PS, and 0.1 M ammonium acetate buffer was used as the eluent. The run was performed at 0.5 ml/min. The working detector temperature was 25 °C, and the sensitivity was 512×. Chromeleon software (Dionex) was used for data acquisition and processing (Górska et al., 2016).

Moreover, UV–vis analysis was performed to investigate PS contamination by nucleic acids and proteins (BioPhotometer, Eppendorf).

2.3. Structure analysis

2.3.1. NMR

All NMR data were obtained with a Bruker 600 Hz Avance III spectrometer using a 5 mm QCI probe equipped with a z-gradient. TopSpin 3.1pl6 software was used for data acquisition, while TopSpin 4.0.7 and SPARKY were used for spectra processing (Lee et al., 2015). For analysis, 5 mg of lyophilized PSs were dissolved in deuterium oxide and placed in 5 mm NMR tubes. Each sample was subjected to one- (^{1}H, ^{31}P) and two-dimensional NMR experiments (^{1}H–^{1}H-COSY, ^{1}H—^{1}H TOCSY, ^{1}H—^{1}H NOESY, ^{1}H—^{13}C HSQC, ^{1}H—^{13}C HMBC, ^{1}H—^{31}P HSQC, and ^{1}H—^{13}C HSQC-TOSCY) using pulse sequences from the Bruker library. Several mixing times were used for TOCSY (30, 60, 100 ms) and NOESY (100, 300 ms) experiments. Diffusion-Ordered Spectroscopy (DOSY) was performed using the ledbpgp2s pulse sequence with a diffusion time of 50 ms and a gradient length of 2 ms. All the data were collected at 25 °C, and the chemical shifts of the NMR signals were referenced by using acetone as an internal reference (δ_H 2.225 ppm, δ_C 31.05 ppm). The absolute configurations of the monosaccharides were obtained by comparison of their ^{13}C NMR chemical shifts with reference data (Shashkov, Lipkind, Knirel, Kochetkov, 1988a, 1988b).

2.3.2. Chemical analysis

The monosaccharide content was investigated according to the method of Sawardeker et al. (Sawardeker et al., 1965) with modifications as described in our previous studies (Pacyga-Prus et al., 2023). First, 0.3 mg of PS was hydrolyzed with 10 M HCl (80 °C, 25 min). The nitrogen-dried sample was then reduced by overnight treatment with 10 mg/ml $NaBH_4$ at 10 °C, and the reaction was stopped by adding 80 % acetic acid. Free -OH groups were acetylated with methylimidazole and acetic anhydride. Finally, the sugar residues were extracted with a water : dichloromethane (1:1, *v*/v) mixture, and the organic phase was collected.

The monosaccharide linkage and substitution positions were obtained by methylation analysis. Briefly, NaOH was added to 2 mg of PS in DMSO, and the mixture was sonicated. The sample was then cooled, iodomethane was added, and the mixture was vortexed (3 × 3 min). Then, the neutral pH was restored with 1 M acetic acid, and methylated sugars were extracted 3 times with a mixture of chloroform and water (1:1, v/v) (Ciucanu & Kerek, 1984). The organic phase was collected and dried under a nitrogen stream. Then, the sample was treated with 10 M HCl, reduced with $NaBH_4$, and neutralized with 80 % acetic acid as described for the sugar analysis. The methylated sugars were extracted with a water : dichloromethane (1:1, v/v) mixture, and the organic phase was collected.

The samples obtained after sugar and methylation analyses were dried under a nitrogen stream and kept at 4 °C until further investigation. For gas–liquid chromatography–mass spectrometry (GLC-MS), the samples were dissolved in ethyl acetate. The analysis was performed on an ITQ 700 Thermo Focus GC system equipped with a Zebron ZB-5HT Inferno capillary column (Phenomenex) with a temperature gradient from 150 °C to 270 °C (8 °C/min). All the data were obtained and analyzed with Xcalibur™ software (Thermo Fisher). Additionally, sugar standards were tested with the samples after sugar analysis to verify the monosaccharide content.

2.3.3. Carbohydrate structure database analysis

The structural units of B.PAT and B.MAT were encoded and pasted to the Carbohydrate Structure Database (CSDB) to confirm that their unique structure was not previously described (as of 15.03.2024) (Toukach, 2011). Additionally, a Structure Editor (a part of CSDB) was used to visualize 3D models of the isolated PS (as of 15.03.2024) (Bochkov & Toukach, 2021).

2.4. Mouse cell isolation and stimulation

To investigate the immunomodulatory properties of the isolated PSs, bone marrow dendritic cells (BMDCs) precursors were isolated from 8- to 10-week-old naïve female BALB/c mice according to methods commonly used in our laboratory (Górska et al., 2014; M. J. Pyclik et al., 2021). For the procedure, the mice were euthanized by cervical dislocation after 3 % isoflurane anesthesia. All experiments were performed following the EU Directive 2010/63/EU for animal experiments. Animal experiments were approved by the Committee for the protection and use of experimental animals of the Institute of Microbiology, The Czech Academy of Sciences (No. 91/2019).

BMDCs were prepared as previously described (Górska et al., 2014). Briefly, femurs and tibias were cleaned from skin and muscles, and cells were rinsed from bones with the use of RPMI 1640 medium. Cells were seeded on a Petri dish in an RPMI 1640 medium (4 × 10^6 cells/plate) supplemented with 10 % FBS, 100 U/ml penicillin, 100 μg/ml streptomycin, 10 mM HEPES and 20 ng/ml murine granulocyte-macrophage colony-stimulating factor (GM-CSF, Invitrogen). Precursor cells were differentiated for one week with the addition of fresh medium on the 3rd and 6th day. On the 7th day, BMDCs were collected from Petri dishes, counted, and seeded on a 96-well plate (0.5 × 10^6 cells per well). Next, the cells were treated with the studied PSs (30 and 90 μg/ml) alone or in combination with *Lacticaseibacillus rhamnosus GG* (10:1, bacteria : BMDCs). Non-stimulated cells were used as a negative control, and cells treated with 1 μg/ml ultra-pure LPS (Invivogen) served as a positive control. BMDCs were incubated for 20 h at 37 °C and 5 % CO_2. The levels of the cytokines IL-10, IL-6, IL-12p70, and TNF-α in culture supernatants were detected with ELISA (Ready-Set-Go! Kits (eBioscience) according to the manufacturer's instructions. Moreover, cells after stimulation with B.PAT and B.MAT (30 μg/ml and 120 μg/ml) were subjected to cytotoxicity analysis *via* the SRB assay (Vichai & Kirtikara, 2006). Briefly, after stimulation, the cells were fixed with 10 % trichloroacetic acid and left at 4 °C for 1 h. Next, the plate was washed four times with water, and 0.06 % sulforhodamine B was added to dye the cells (30 min, RT, in darkness). Finally, the plate was washed four times with 1 % acetic acid to remove the excess dye, and the remaining protein-bound reagent was dissolved in 10 mM Tris base solution (pH = 10.5). Finally, the absorbance was read at 490, 510, and 530 nm.

2.5. Human cell lines stimulation in the IL-1β inflammatory model

The adherent, immortalized epithelial cell lines of male human colorectal adenocarcinoma (Caco-2) and the female human, adherent, immortalized epithelial colon cancer cell line (HT-29) were used (after the 10th passage) to test the potential anti-inflammatory properties of B. PAT and B.MAT. First, 0.5 × 10^6 cells/well were seeded on a 12-well plate in DMEM/F12 (Gibco) supplemented with 10 % FBS (Gibco) and a 1 % L-glutamine-Penicillin-Streptomycin solution for HT-29 cells, and EMEM/DMEM high glucose (Sigma Aldrich) supplemented with 10 % FBS, 1 × non-essential amino acids (100 × concentrated, Sigma Aldrich), and 10 mM HEPES (Sigma Aldrich) for Caco-2 cells. After, the Caco-2 cells were incubated for 24 h, and the HT-29 cells were allowed to adhere to the plate for 48 h.

2.5.1. Prophylactic model

The cells adherent to the plate were stimulated with B.PAT and B. MAT at a 10 μg/ml concentration. The cells were incubated for 18 h (37 °C, 5 % CO_2). Then, 10 ng/ml IL-1β was added to the cells, and after an additional 18 h of incubation (37 °C, 5 % CO_2), the media above the cells were collected and frozen. Finally, to measure the levels of IL-8 in culture supernatants, an ELISA Ready-Set-Go! Kit (BD Biosciences) was used according to the manufacturer's instructions.

2.5.2. Therapeutic model

The cells adherent to the plate were stimulated with 10 ng/ml IL-1β. The cells were incubated for 18 h (37 °C, 5 % CO_2). Then, B.PAT and B. MAT were added to the cells, and an additional 18 h of incubation (37 °C, 5 % CO_2) was performed. The media above the cells were collected and frozen. Finally, to measure the levels of IL-8 in culture supernatants, an ELISA Ready-Set-Go! Kit (BD Biosciences) was used according to the manufacturer's instructions.

2.6. Statistical analysis

All experiments were repeated with at least two technical and two biological repetitions. The data were presented as the mean ± SD and differences were analyzed with an unpaired *t*-test. All the statistical analyses and visualizations were prepared with Graph Pad Prism version 9.

3. Results

3.1. Structural analysis of B.PAT polysaccharide

B.PAT was separated from a complex PS blend that was isolated from the surface of the Ba218 strain. The crude PS mixture was submitted to ion exchange and size exclusion chromatography and subsequently analyzed by NMR spectroscopy. This led to the determination of the three distinct PS fractions. The ^{31}P NMR spectra showed that B.PAT was the only PS containing phosphorus in its structure. Since the main idea behind this study was to investigate changes in the immunomodulatory properties of phosphorylated PSs and their dephosphorylated counterparts, the phosphate-substituted B.PAT was selected for further experiments.

Sugar analysis indicated that B.PAT consists of L-Rha, D-Glc, and D-Gal in a molar ratio of 1:1.5:3. An average molecular mass of *ca.* 1.96 × 10^4 Da was determined.

Analysis of the ^{1}H—^{13}C HSQC spectrum showed 12 cross peaks in the anomeric region. Since some of the signals in the ^{1}H NMR spectrum and in the 2D HSQC spectrum were significantly broader than others, DOSY experiments that allow the separation of molecules based on their different sizes or mobilities were performed (Fig. 1, Supplementary Fig. S1).

The DOSY spectra showed that the B.PAT PS consists of a non-asaccharide repeating unit with 8 hexapyranosyl and 1 hexafuranosyl residues as determined from the ^{1}H—^{13}C HSQC NMR spectrum (Fig. 2).

The structure of the PS was obtained from analysis of the 2D NMR spectra, including COSY, TOCSY, and NOESY at several mixing times, HSQC, HSQC-TOCSY, and HMBC (Supplementary Fig. 2–5). In Table 1, the sugar residues of B.PAT are marked with an uppercase letter starting from the most downfield signal in the ^{1}H NMR spectrum.

Analysis of the TOCSY and HSQC-TOCSY spectra allowed us to determine the type of sugar residues constituting B.PAT. Residue A was assigned as a hexafuranose due to the strong downfield shift of the anomeric carbon signal with the *galacto*-configuration. For residues B, C, E, and F, the characteristic methyl resonances of 6-deoxy sugars were observed at 1.28, 1.33, 1.32, and 1.26, respectively. In the TOCSY spectra, only one cross-peak was found between H1 and H2 of those residues, indicating that they are rhamnoses. Therefore, the spin systems for residues B, C, E, and F were obtained from the TOCSY and HSQC-

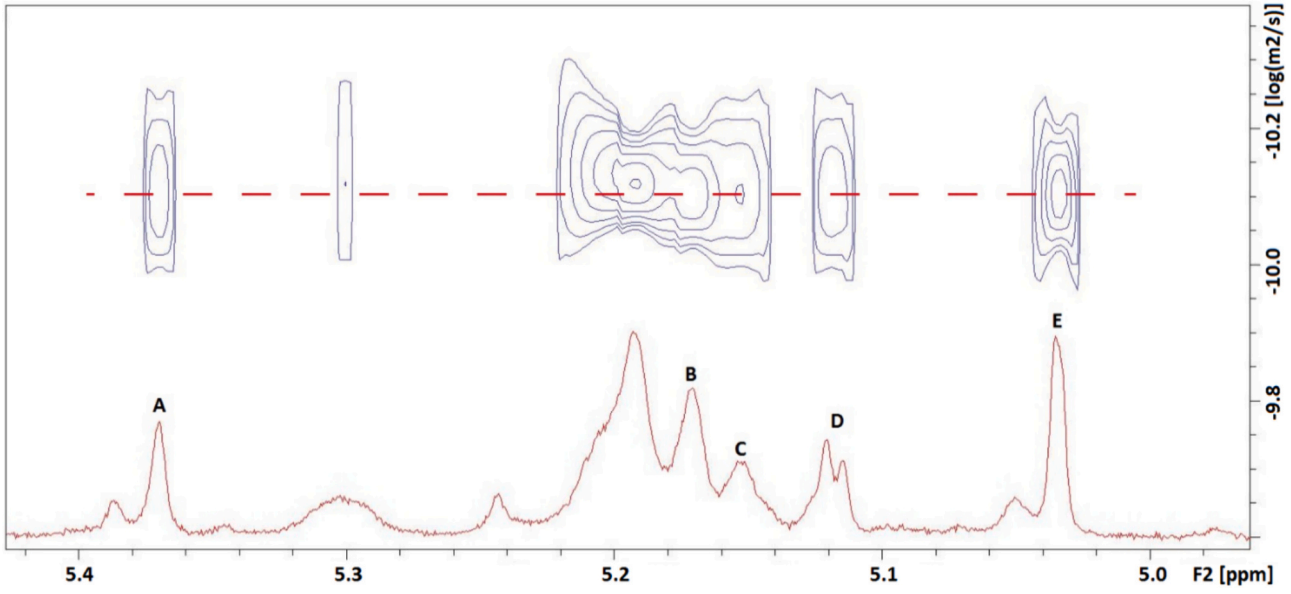

Fig. 1. A part of the DOSY spectrum of B.PAT showing the anomeric region of the PS (blue). The experimental ^{1}H NMR spectrum is shown in red. Signals on the same level (red, dashed line) belong to B.PAT structure (marked as A-E).

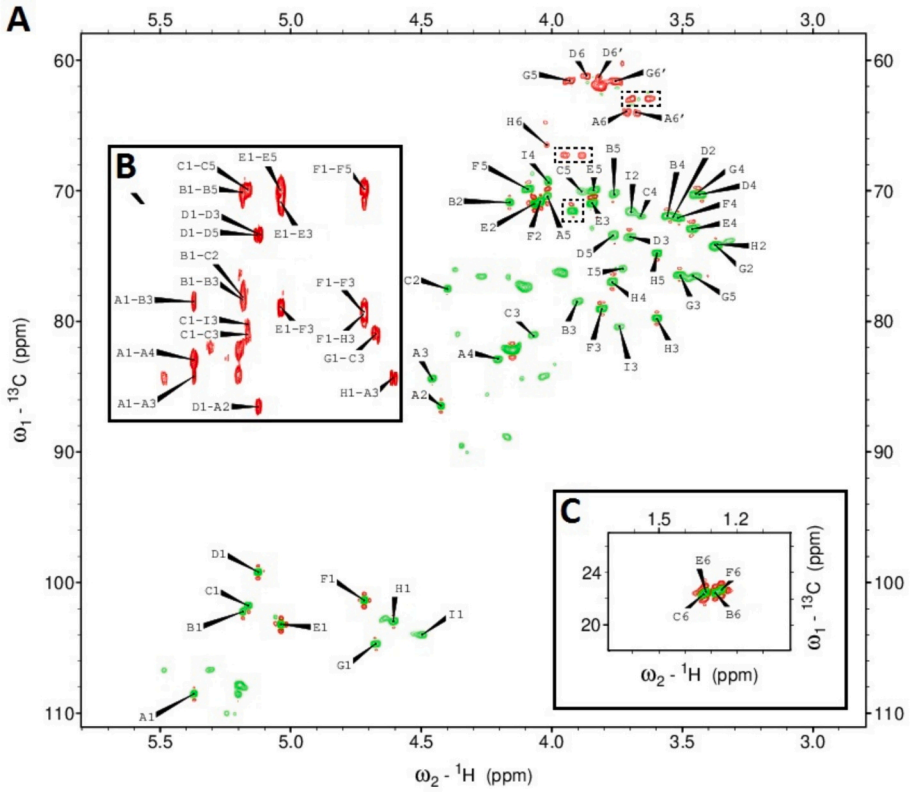

Fig. 2. A. Part of the $^{1}H—^{13}C$ HSQC NMR spectrum of B.PAT at 25 °C. The anomeric signals are located in the chemical shift range of 4.2–5.8 ppm and the ring signals are between 3.2 and 4.5 ppm. The black dashed line indicates the signals corresponding to the glycerol substitution. B. The part of the HMBC spectrum corresponds to the anomeric signals in the HSQC spectra. C. H-6/C-6 signals for rhamnoses (residues B, C, E, and F).

TOCSY spectra using the methyl groups as starting points. An analysis of scalar correlations for residues D, G, and H showed resonances characteristic for the *gluco*-configuration. Finally, residue I was assigned to the *galacto*-configuration since the analysis of the TOCSY and HSQC-TOCSY spectra showed scalar correlations from the anomeric signal only until the H4/C4 resonance. The H5/C5 chemical shifts for residue I were determined from the connectivity between H3 and H5 in the NOESY spectra and from the connectivity between H1 and C5 in the HMBC spectrum.

The anomeric configuration of residue A was identified as β due to the downfield shift of the anomeric carbon lower than δ 105 ppm, which is observed only for the β-configuration of galactofuranoside (Gorin & Mazurek, 1975; Nagaoka et al., 1996). For the rhamnoses (residues B, C, E, and F) the $^{3}J_{H1H2}$-values were small (< 3.0 Hz) and not resolved in the NMR spectra due to line broadening and therefore could not be used to determine the anomeric configuration. However, it has been shown that the chemical shift of the C5 signal can be used to distinguish between α- or β-linkages. The C5 resonance at δ 70.5 ppm indicates the α-configuration, while the C5 resonance at δ 73.2 ppm is attributed to the β-configuration (Carillo et al., 2009; Lipkind et al., 1988; Mattos et al., 2001; Senchenkova et al., 1999; Vinogradov et al., 2003). Since residues B, C, E, and F have C5 resonances <70.5 ppm, they were assigned as α-rhamnoses. The α-configuration was also confirmed by the absence of intraglycosidic NOEs between H1 and H3, H5 (Vinogradov et al., 2003). The glucose residues G, H, and galactose I have $^{3}J_{H1H2}$-values >7 Hz, indicating a β, while residue D, with a small $^{3}J_{H1H2}$-value of 3 Hz, was assigned an α. The chemical shift of C6 from the H residue could not be assigned unambiguously due to the lack of scalar connectivities between H5/C5 and H6/C6. The reason might be that the C-6 substitution by glycerol phosphate affects the conformation around the C5-C6 bond.

The connections between the monosaccharides in the B.PAT unit were determined from NOESY and HMBC spectra (Table 2). The glycosylation pattern was further confirmed by the downfield shift of signals belonging to C2 and C3 of Gal*f* (A), C3 of Rha*p* (B), C2 and C3 of Rha*p* (C), C3 of Rha*p* (F), C3 and C4 of Glc*p* (H), and C3 of Gal*p* (I) compared to those of the non-substituted sugars. Moreover, a strong downfield shift was observed for the C6 signal of Glc*p* (H), indicating substitution at this position. Analysis of the $^{1}H—^{13}C$ HSQC spectrum together with the $^{1}H—^{31}P$ HSQC spectrum revealed that phosphorus substituted both glycerol at 3.95 and 3.88 ppm (δ 67.3 ppm, glycerol) and H6 at 4.02 and 4.07 ppm (δ 66.4 ppm, residue H).

The absolute configuration of B.PAT monosaccharide moieties was tentatively obtained from the ^{13}C NMR chemical shifts and compared with reference data (Shashkov, Lipkind, Knirel, Kochetkov, 1988a). Thus, the following sequence for the B.PAT's repeating unit was proposed: →2)-[β-D-Glc*p*-(1 → 3)-]α-L-Rha*p*-(1 → 3)-β-D-Gal*p*-(1 → 4)-[D-Gro(→P → 6)-,α-L-Rha*p*-(1 → 3)-]α-L-Rha*p*-(1 → 3)-]β-D-Glc*p*-(1 → 3)-[α-D-Glc*p*-(1 → 2)-]β-D-Gal*f*-(1 → 3)-α-L-Rha*p*-(1→, or with the uppercase letters: [G-]C-I-[Gro-P-,*E*-F-]H-[D-]A-B. The obtained structure was consistent with the methylation analysis results, thus, the proposed structure of the repeating unit was proposed (Fig. 3).

To better understand the influence of phosphorylation on B.PAT, it underwent dephosphorylation for 48 h at 4 °C. The dephosphorylation process was confirmed by ^{31}P NMR experiments. Analysis of 2D NMR spectra allowed us to assess the impact of glycerol phosphate on B.PAT structure (Fig. 4).

Dephosphorylation of B.PAT did not affect the main chain of PS. Differences between the B.PAT and B.MAT structures focus on residue H only and lead to changes in the HSQC, TOCSY, and HSQC-TOCSY spectra, confirming that phosphorylation is related to this sugar in B.PAT's repeating unit (Table 3). However, even after dephosphorylation, chemical shifts for C6 of residue H could not be assigned unambiguously.

Moreover, a search in an online database (CSDB) confirmed that the

Table 1
^{1}H and ^{13}C NMR chemical shifts of the resonances of B.PAT from *Bifidobacterium animalis* ssp. *animalis* CCDM 218.

		^{1}H, ^{13}C chemical shifts (ppm)					
Sugar residue		H-1, C-1	H-2, C-2	H-3, C-3	H-4, C-4	H-5, C-5	H-6, H-6′ C-6
A	→2,3)-β-D-Gal*f*-(1→	5.37 108.5	4.42 86.5	4.45 84.4	4.21 82.9	4.02 70.4	3.71, 3.67 64.0
B	→3)-α-L-Rha*p*-(1→	5.18 102.2	4.16 70.9	3.90 78.5	3.54 71.9	3.76 70.3	1.28 17.5
C	→2,3)-α-L-Rha*p*-(1→	5.16 101.8	4.4 77.5	4.07 81.0	3.66 72.0	3.89 70.1	1.33 17.6
D	α-D-Glc*p*-(1→	5.12 99.2	3.56 71.9	3.70 73.5	3.44 70.3	3.76 73.4	3.82, 3.86 61.3
E	α-L-Rha*p*-(1→	5.04 103.2	4.07 71.0	3.85 70.9	3.46 72.9	3.84 70.0	1.32 17.5
F	→3)-α-L-Rha*p*-(1→	4.72 101.3	4.04 70.8	3.81 79.0	3.52 72.1	4.09 69.8	1.26 17.3
G	β-D-Glc*p*-(1→	4.68 104.7	3.37 74.2	3.51 76.4	3.44 70.3	3.46 76.6	3.75, 3.93 61.6
H	→3,4,6)-β-D-Glc*p*-(1→	4.61 103.0	3.37 74.2	3.60 79.7	3.77 77.0	3.60 74.8	4.02, 4.07 66.4
I	→3)-β-D-Gal*p*-(1→	4.5 104.0	3.7 71.6	3.74 80.4	4.01 69.3	3.73 76.0	
	Glycerol phosphate	3.69, 3.63 62.9	3.92 71.5	3.95, 3.88 67.3			
	^{31}P	0.7					

Table 2
Selected inter-residue correlations from ^{1}H—^{1}H NOESY and ^{1}H—^{13}C HMBC spectra of B.PAT.

		H-1 / C-1	Connectivity to		Inter-residue
	Residue	δ_H / δ_C	δ_C	δ_H	Atom / Residue
A	→2,3)-β-D-Gal*f*-(1→	5.37 / 108.5	78.5	3.90	C-3, H-3 of B
B	→3)-α-L-Rha*p*-(1→	5.18 / 102.2	81.0	4.07	C-2, H-2 of C
C	→2,3)-α-L-Rha*p*-(1→	5.16 / 101.8	80.4	3.74	C-3, H-3 of I
D	α-D-Glc*p*-(1→	5.12 / 99.2	86.5	4.42	C-2, H-2 of A
E	α-L-Rha*p*-(1→	5.04 / 103.2	79.0	3.81	C-3, H-3 of F
F	→3)-α-L-Rha*p*-(1→	4.72 / 101.3	79.7	3.60	C-3, H-3 of H
G	β-D-Glc*p*-(1→	4.68 / 104.7	81.0	4.07	C-3, H-3 of C
H	→3,4,6)-β-D-Glc*p*-(1→	4.61 / 103.0	84.4	4.45	C-3, H-3 of A
I	→3)-β-D-Gal*p*-(1→	4.5 / 104.0	70.8	4.04	C-4, H-4 of H
	Glycerol phosphate	3.95, 3.88 / 67.3	66.4	4.02, 4.07	C-6, H-6 of H

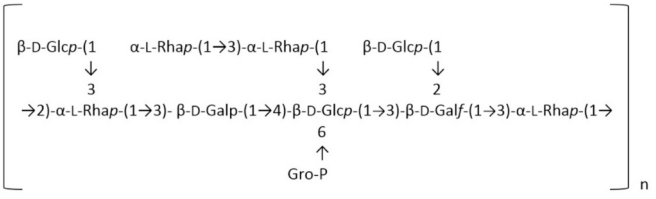

Fig. 3. Structure of the nonasaccharide repeating unit of B.PAT. The approximate number of units in B.PAT equals $n = 7$.

structure of B.PAT and B.MAT were not described previously. The CSDB Structure Editor allowed the prediction of 3D models of both PSs variants. The obtained 3D models indicate that the loss of Gro-P in dephosphorylated PS affects the spatial structure of B.PAT with a more open structure, which may influence the differences in the properties of both PSs (Fig. 5).

Finally, UV–vis analysis was performed to ensure that the PS fractions were free of nucleic acid and protein contamination (Supplementary Table T1).

3.2. Distinct immunomodulatory properties of B.PAT and B.MAT

A strong, dose-dependent production of TNF-α, IL-6, and IL-10 cytokines was the result of BMDCs stimulation with B.MAT (Fig. 6A). Furthermore, B.MAT was the only one able to induce IL-12 production at 90 μg/ml. B.PAT, on the other hand, induced low levels of IL-6 and TNF-α without inducing IL-10 or IL-12 production. To confirm the distinct modulatory properties of B.PAT and B.MAT, BMDCs were stimulated with a strain known for its immunomodulatory properties – *Lacticaseibacillus rhamnosus* GG – with the addition of the studied compounds (Fig. 6B). Both B.PAT and B.MAT were able to enhance cells' response to stimulation with the selected strains in a dose-dependent manner for isolated PSs as well as in favor of the dephosphorylated compound. A significantly greater production of TNF-α (** $p \leq 0.01$) was observed for B.MAT at the highest concentration in comparison to B.PAT (when stimulated with a lactobacilli strain). Moreover, B.MAT at 90 μg/ml in the same variant of the experiment showed a stronger tendency than B.PAT to intensify IL-12 and IL-10 production. No differences in enhancing lactobacilli strain immunomodulatory properties were observed for either PS for IL-6 levels.

Moreover, the viability assay confirmed the safety of B.PAT and B.MAT, since the survival rate did not significantly differ between the control cells (untreated cells, 100 %) and the cells treated with the tested PSs (Supplementary Fig. S6).

3.3. Dephosphorylation enhances the anti-inflammatory properties of B.PAT

To fully understand the potential of B.PAT and B.MAT, their anti-inflammatory properties were tested in Caco-2 and HT-29 cells. Both cell lines are widely used as models of the intestinal epithelial barrier in which inflammation is induced with the use of IL-1β. Isolated PSs were administered before (prophylactic) or after (therapeutic) IL-1β treatment to investigate their possible role in the prevention or treatment of inflammatory responses. Notably, the phosphorylated compound was able to inhibit the development of inflammatory responses in prophylactic settings, which resulted in lower levels of IL-8 in both HT-29 cells and Caco-2 cells. Dephosphorylation significantly enhanced the ability of B.PAT to prevent inflammation by even stronger suppression of IL-8 production in both cell lines (** $p \leq 0.01$ for HT-29 cells and * $p \leq 0.05$ for Caco-2 cells). Moreover, B.MAT showed a tendency to reduce IL-8 production in HT-29 cells in therapeutic settings after stimulation with IL-1β (Fig. 7) ($p = 0.09$, in comparison to the IL-1β control).

4. Discussion

The presented study was based on the idea that modifications of PSs can greatly influence their functions. To prove this hypothesis, PSs were isolated from the surface of *Bifidobacterium animalis* ssp. *animalis* CCDM 218 and purified by chromatography methods. The obtained fractions were subjected to NMR analysis, which showed that one of the structures, B.PAT, is phosphorylated. The first step in understanding the presence of phosphorus on B.PAT was to determine the PS structure. Studies of human-derived *Bifidobacterium* strains have shown that the typical size of bifidobacterial PSs is between 10^4 and 10^6 Da and that the most common sugars that build a PS chain unit are glucose, galactose,

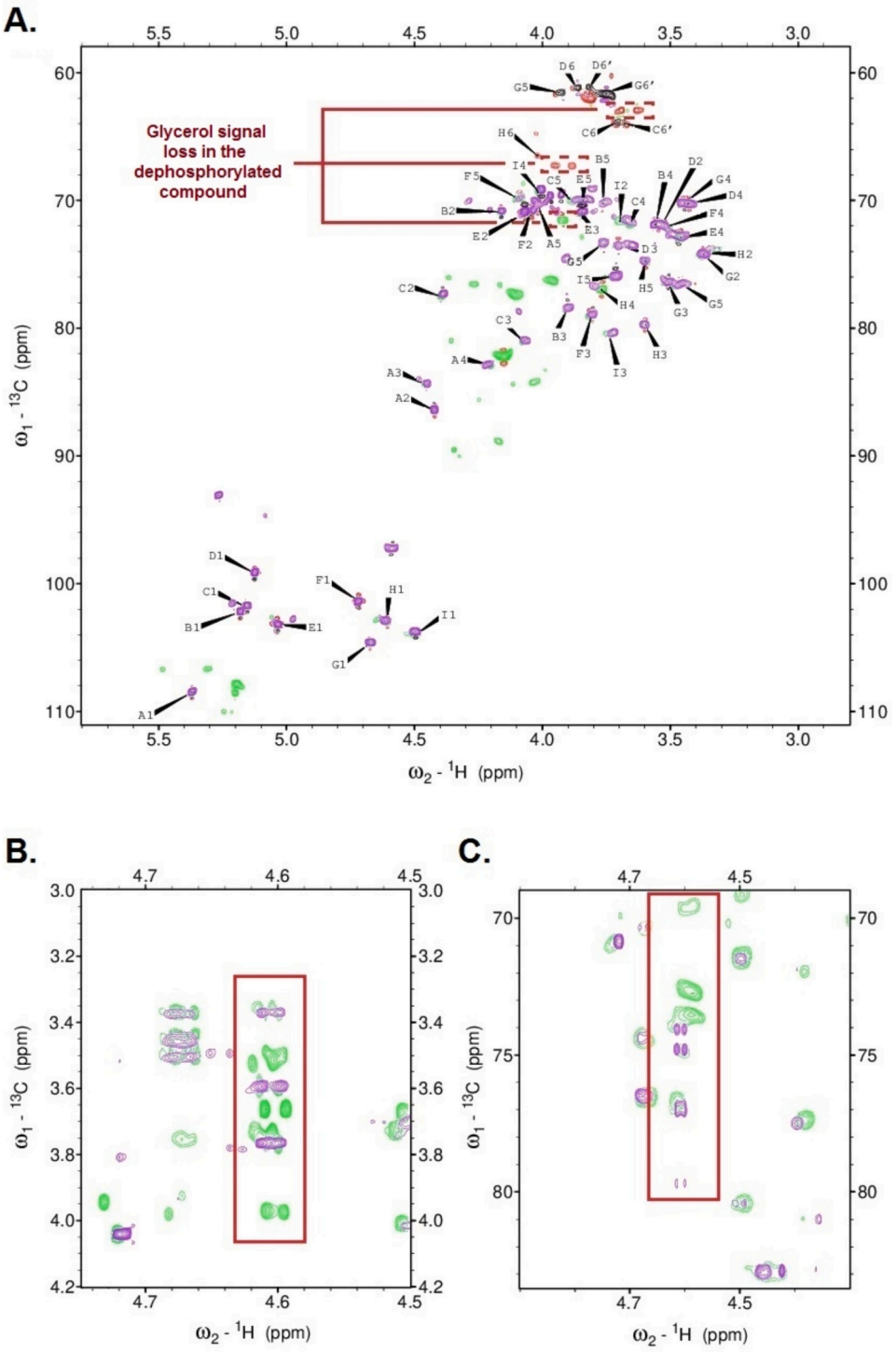

Fig. 4. Differences between B.PAT and B.MAT. A. Overlapped $^{1}H—^{13}C$ HSQC spectra of B.PAT and B.MAT. There is a loss of glycerol signals (red, dashed line) in the dephosphorylated compound, as well as a loss of additional signals present in B.PAT. B. Overlapped TOCSY spectrum of the residue H region of B.PAT and B.MAT (red box). C. Overlapped HSQC-TOCSY spectrum of residue H region of B.PAT and B.MAT (red box). The green and red spectra correspond to B.PAT, while purple and black ones – to B.MAT.

and rhamnose (Salazar et al., 2009). B.PAT is a small PS of 1.96×10^4 Da, and sugar analysis revealed the presence of only glucose, galactose, and rhamnose in its structure. The small size of the PS may be the first indicator of its possible properties. As described previously by Górska et al. (2014), PSs with small molecular sizes are associated with pro-inflammatory responses, while PSs with high molecular masses exhibit regulatory properties (Górska et al., 2014). Given the relatively small molecular mass of our PSs, we also considered them to have pro-inflammatory properties. In contrast to the findings of Górska et al., our results obtained in the IL-1β inflammatory model showed prophylactic effects of both B.PAT and B.MAT, indicating their anti-inflammatory effect. Therefore, the function of PS might be based not only on its size and sugar composition but also on the molar ratio of its components, the order of sugars in a PS chain unit, the spatial structure, and, most importantly, on the non-sugar substitutions of the PS chain. The structure determination of B.PAT revealed a highly branched PS

Table 3
Comparison of the B.PAT's and B.MAT's differences in chemical shifts for residue H.

Sugar residue		^{1}H, ^{13}C chemical shifts (ppm)					
		H-1, C-1	H-2, C-2	H-3, C-3	H-4, C-4	H-5, C-5	H-6, H-6' C-6
B.PAT							
H	→3,6)-β-D-Glc*p*-(1→	4.61 103.0	3.37 74.2	3.60 79.7	3.77 77.0	3.60 74.8	4.02, 4.07 66.4
B.MAT							
H	→3)-β-D-Glc*p*-(1→	4.61 102.9	3.36 73.8	3.6 79.7	3.80 76.75	3.54 71.82	

with 4 rhamnose, 3 glucose, and 1 galactose residues in the pyranose form, and 1 galactose residue in the furanose form. Most of its sugar residues have an alpha configuration, and there is a majority of 1 → 3 glycosidic bonds that positively influence the flexibility of PS and may result in increased anti-microbial and anti-oxidant properties (Laws et al., 2001; Zhou et al., 2019). Moreover, chemical modifications can greatly improve the spatial configuration of PS and influence its physiological properties and functions. There is a broad spectrum of modifications that can occur on the PS chain, including acetylation, sulfation, and phosphorylation. B.PAT was found to be substituted by glycerol phosphate connected to β-D-Glc*p* (residue H) at the 6th position. Phosphorylated PSs, such as B.PAT, are not abundant in nature, and the degree of substitution in a phosphorylated PS is usually low. Phosphorus-containing PSs are often more complex, and their structure is difficult to determine (Laffargue et al., 2023). There are even fewer examples of glycerol phosphate substitutions in bacterial PSs. Edgar et al. (2019) described *Streptococcus mutans* rhamnose PSs that contain glycerol phosphate modifications on approximately 25 % of the GlcNAc residues (Edgar et al., 2019). Furthermore, Speciale et al. (2019) described an 8 × 10^4 Da phospho-glycero-β-galactofuronian (PGβG) substituted by glycerol phosphate at the 6th position and produced by *Bifidobacterium bifidum* PRI1 (Speciale et al., 2019).

To better understand the role of glycerol phosphate substitution on B.PAT, the PS was dephosphorylated. Comparison of NMR data for B.PAT (with phosphorus) and B.MAT (after dephosphorylation) showed that dephosphorylation caused significant changes in the chemical shifts of the carbons belonging to the residue, which is consistent with the literature data (Fig. 4, Table 3) (Kołodziejska et al., 2006; Speciale et al., 2019). Further investigation of the 3D models predicted by the Structure Editor showed that the loss of glycerol phosphate substitution may result in spatial changes in isolated PSs, and the structure became less condensed since the H residue lost its substitution at the C6 position (Fig. 5). This may be the cause of better recognition of B.MAT and increased cytokine production in the tested cells.

Liu et al. (2023) discussed in detail the impact of phosphorylation on PSs and emphasized that adding phosphorus to the structure can lead to spatial changes and affect PSs function (Liu et al., 2023). Few publications have compared the functions of phosphorylated and dephosphorylated PSs. Even fewer studies have expanded their research by structure investigation. The majority of related research indicates that the phosphorylation of PSs results in an improvement in their activity. Neutral (NPS) and phosphorylated (APS) PSs were described for *Lactobacillus delbrueckii* ssp. *bulgaris* OLL1073E-1. Both consist of the same structure with galactose and glucose residues in a molar ratio of 3:2 (Nishimura-Uemura et al., 2003). The only difference was the presence of 0.1 % phosphorus in the APS fraction. Studies performed on the mouse macrophage-like cell line J774.1 revealed that APS is a stronger immunomodulator than NPS, as it can significantly increase IL-6, IL-10, and IL-12p40 while decreasing IL-12p35 levels. To prove that the effect of APS is caused by the presence of phosphorus substitution, APS was subjected to dephosphorylation, which led to the inhibition of its mitogenic and cytostatic activity (Nishimura-Uemura et al., 2003). Another immunomodulatory effect was observed by Makino et al. (2006), who isolated neutral (NPS) and phosphorylated (H-APS) high molecular mass PSs from the same strain as Nishimura-Uemura et al. These PSs consisted of glucose, galactose, mannose, and xylose (for NPS) and glucose, galactose, and 0.01 % phosphorus substitution (for H-APS). In C3H/HeJ mouse spleen cells, compared with NPS, APS caused a significant increase in IFN-γ. Moreover, *in vivo* analysis of murine splenocytes isolated from BALB/c mice previously administered with H-APS revealed a dose-dependent increase in NK cell induction. Furthermore, compared with the control treatment, treatment with concanavalin A positively affected the production of IFN-γ and the inhibition of IL-4 (Makino et al., 2006). Another interesting example is the introduction of phosphorus to dextran at a degree level of 1.7–2 %. It induced mitogenic activity in mouse splenocytes. In addition, it was able to induce the expression of CD86 as well as the gene expression of IL-10 and IFN-γ in comparison to non-phosphorylated dextran (Sato et al., 2004). However, dephosphorylation is not always associated with the suppression of PS function. Speciale et al. (2019) isolated surface PSs from *Bifidobacterium bifidum* PRI1 that led to the purification of structurally different fractions. The first fraction contained at least 4 different β-glucan/galactan PSs with an average molecular mass of 4 × 10^4 Da (CSGG). The second one was determined to be phosphor-glycero-β-galactofuronian (PGβG), which has an average molecular mass of 8 × 10^4 Da. Studies investigating CSGG and PGβG activities have shown that the neutral fraction can induce Foxp3$^+$ cells in spleen-derived mouse DCs. Moreover, CSGG improved the production of IL-10, suggesting that this PS has regulatory properties (Speciale et al., 2019). This effect was confirmed by Verma et al. (2018), who described the suppressive effect of this PS on the development of colitis in mice. In contrast, the

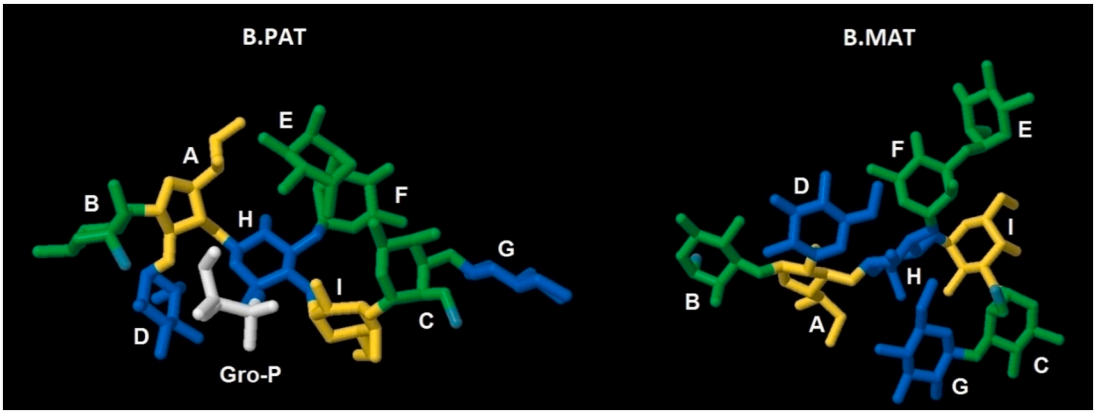

Fig. 5. 3D models of B.PAT and B.MAT predicted by CSDB Structure Editor. After dephosphorylation, the spatial structure of B.PAT is significantly changed.

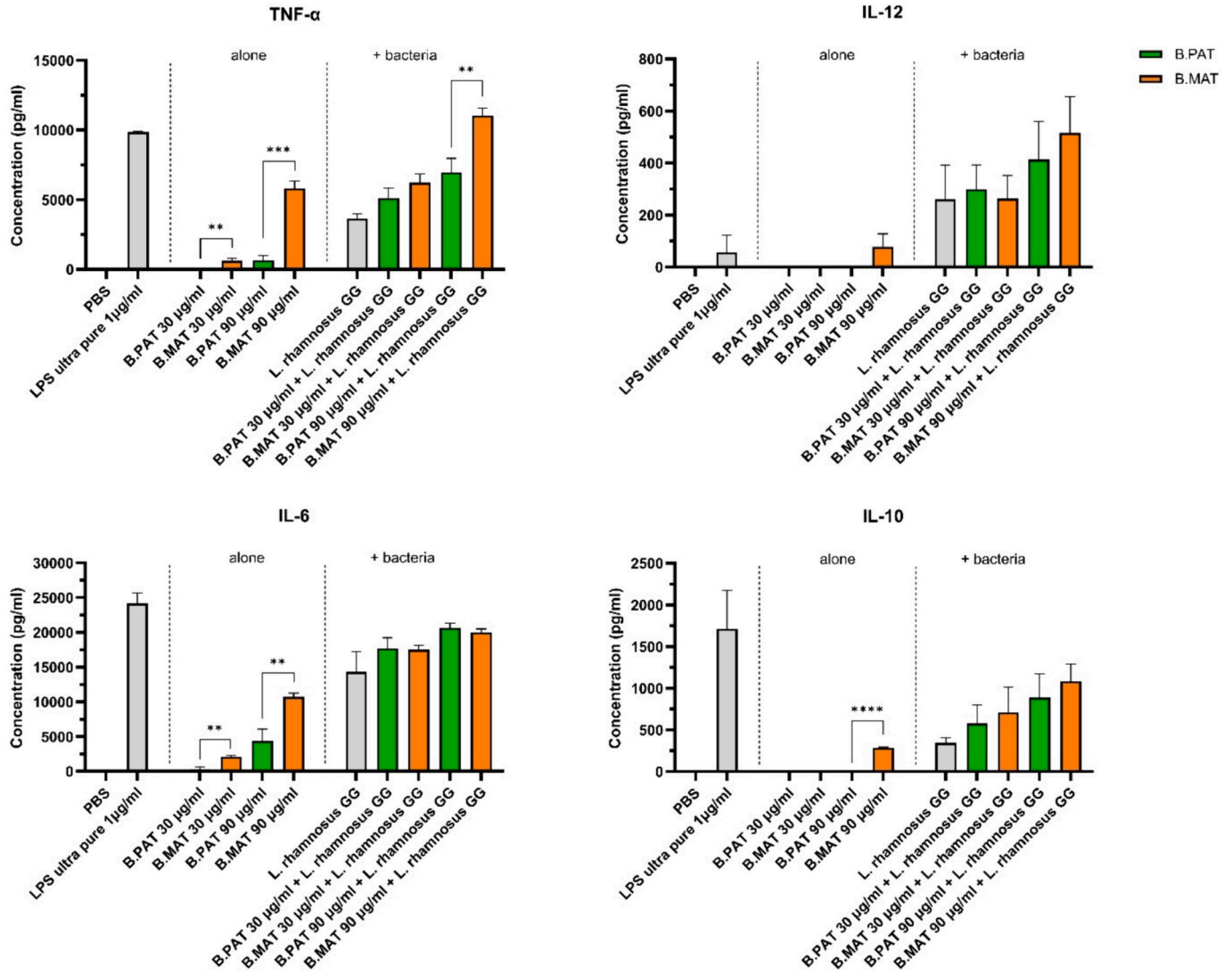

Fig. 6. Cytokine production after immune cells stimulation with B.PAT and B.MAT. Mouse BMDCs stimulation with PBS (negative control), LPS ultra-pure (positive control, Invivogen), or PSs at a concentration of 30 and 90 μg/ml alone or with the addition of *Lacticaseibacillus rhamnosus* GG. B.PAT was marked in green, while B.MAT was marked in orange. An unpaired *t*-test was performed, and significant differences between phosphorylated and dephosphorylated compounds (90 μg/ml) were calculated (**** $p \leq 0.0001$, *** $p \leq 0.001$, ** $p \leq 0.01$).

phosphorylated fraction did not affect Foxp3^{+} expression, however, it was able to significantly increase IFN-γ levels, while IL-10 remained unaffected. This may indicate that, unlike regulatory CSGG, it has potential pro-inflammatory properties (Verma et al., 2018). Stimulation of mouse BMDCs with isolated PS resulted in significantly greater production of IL-10, IL-6, and TNF-α in response to B.MAT (90 μg/ml) than in response to B.PAT. More interestingly, B.MAT also induced the production of IL-12 at 90 μg/ml, while at the same time, B.PAT was not able to induce either IL-12 or IL-10 at any of the tested doses (Fig. 6A).

To investigate the abilities of B.PAT and B.MAT to enhance the function of known immunomodulators, BMDCs were stimulated with *Lacticaseibacillus rhamnosus* GG, which is known for its health-promoting properties (Capurso, 2019). Both PSs dose-dependently strengthened the effect of the whole bacteria. However, greater cytokine production was observed after the addition of dephosphorylated PS, which is consistent with previous results (Fig. 6B). In the case of IL-10 and IL-12 production, B.PAT alone was not capable of inducing high levels of these cytokines at the tested doses. Simultaneously, B.MAT induced low IL-10 and IL-12 levels at 90 μg/ml. However, stimulation with lactobacilli proved that both PSs can act as costimulators of different antigens, improving the effect of other known immunomodulators. Górska et al. (2014) described two PSs from *Lacticaseibacillus rhamnosus* LOCK 900 (Górska et al., 2014). Both were negatively charged, but L900/2 was a large (8.3×10^6 Da), pyruvylated, branched PS with 7 monosaccharide residues, and L900/3 was a small ($1{,}8 \times 10^4$ Da) PS containing 5 monosaccharides and phosphomonoester substitution. Both PSs were tested in mouse BMDCs together with *Lactobacillus plantarum* WCFS-1. The results showed that the high molecular weight L900/2 PS increased IL-10 production, whereas the small molecular weight L900/3 PS increased IL-12p70 cytokine levels, compared to the strain alone. Thus, the authors indicated that L900/2 might be a possible anti-inflammatory factor in conditions such as inflammatory bowel disease, while L900/3 could play a role in the treatment of allergies (Górska et al., 2014).

To investigate the possible anti-inflammatory properties of isolated PSs, the IL-1β-induced inflammation model was used in Caco-2 and HT-29 human cell lines. IL-1β is known to impair the integrity of intestinal epithelial cells and to enhance the inflammatory response by upregulating IL-8 cytokine production (Al-Sadi & Ma, 2007; Sunil et al., 2010). The addition of isolated PSs prevented the outburst of IL-8 in both HT-29 cells and Caco-2 cells. Interestingly, the dephosphorylated compound had a significantly stronger downregulatory effect on IL-8 production,

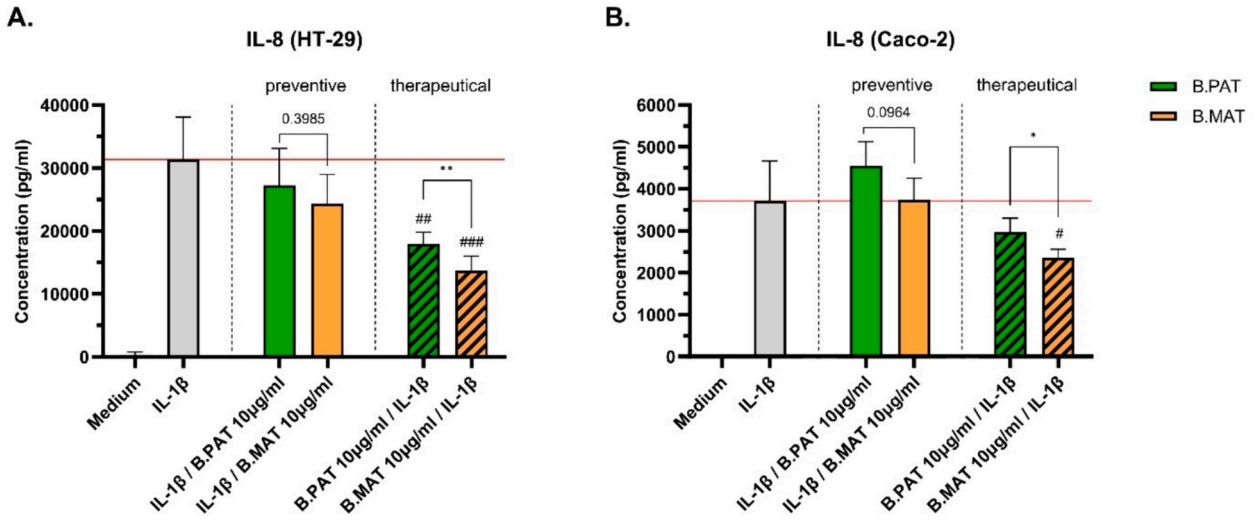

Fig. 7. IL-8 cytokine production after cell lines stimulation with B.PAT and B.MAT. A. Stimulation of HT-29 cell line with tested PS before (preventive) or after (therapeutical) the induction of inflammation with IL-1β. B. Stimulation of Caco-2 cell line with tested PS before (preventive) or after (therapeutical) the induction of inflammation with IL-1β. B.PAT is marked in green, while B.MAT is marked in orange. The red line shows the level of IL-8 after cell treatment with IL-1β only (positive control). An unpaired t-test was performed, and significant differences between phosphorylated and dephosphorylated compounds were calculated (** $p \leq 0.01$, * $p \leq 0.05$). Significance in comparison to positive control was marked with # (### $p \leq 0.001$, ## $p \leq 0.01$, # $p \leq 0.05$).

indicating its anti-inflammatory effects in the presented model.

The immunomodulatory properties of the presented PSs and, in particular, the dephosphorylated B.MAT molecule show potential for future use in the prevention or treatment of various diseases. The greatest advantages of these molecules are the well-described structures introduced in this research. Moreover, the knowledge presented in this manuscript provides a strong foundation for future detailed structure–function investigations, which are not possible for whole microorganisms. This approach also provides opportunities for *in vivo* studies. In comparison to probiotics, postbiotics lack virulence factors and cannot transfer antibiotic resistance genes. Overall, their high stability, efficient and easy isolation, and definable structure make them perfect alternatives to probiotics (Rafique et al., 2023).

5. Conclusions

In this work, we comprehensively studied a glycerol phosphate-substituted polysaccharide (PS) called B.PAT isolated from *Bifidobacterium animalis* ssp. *animalis* CCDM 218 and thoroughly described its structure. To fully understand the immunomodulatory potential of B.PAT, we investigated the biological activities of this compound and its dephosphorylated counterpart – B.MAT. The results showed that dephosphorylation strongly influenced the spatial structure of B.PAT. Moreover, studies of BALB/c mouse BMDCs indicated the possible immunomodulatory potential of B.MAT that is stronger than that of B.PAT. Further experiments performed on Caco-2 and HT-29 cells in an IL-1β-induced inflammation model showed the enhanced effect of B.MAT to prevent the development of an inflammatory response. Therefore, our results demonstrated that the dephosphorylation of PSs does not have to be associated with the suppression of PS's function but may also be responsible for the enhancement of the existing properties and different functionalities depending on the tested model.

Funding

This work was supported by the National Science Centre of Poland (UMO-2017/26/E/NZ7/01202); and the Ministry of Education, Youth and Sports of the Czech Republic (CZ.02.01.01/00/22_008/0004597).

CRediT authorship contribution statement

Katarzyna Pacyga-Prus: Writing – original draft, Visualization, Resources, Methodology, Investigation, Formal analysis. **Corine Sandström:** Writing – review & editing, Investigation. **Dagmar Šrůtková:** Writing – review & editing, Resources. **Martin Schwarzer:** Writing – review & editing, Supervision, Resources. **Sabina Górska:** Writing – review & editing, Validation, Supervision, Project administration, Funding acquisition, Conceptualization.

Declaration of competing interest

The authors declare that they have no known competing financial interests or personal relationships that could have appeared to influence the work reported in this paper.

Data availability

Data will be made available on request.

Acknowledgments

Graphical abstract was created using BioRender online software (https://biorender.com/).

Appendix A. Supplementary data

Supplementary data to this article can be found online at https://doi.org/10.1016/j.carbpol.2024.122518.

References

Al-Sadi, R. M., & Ma, T. Y. (2007). IL-1β causes an increase in intestinal epithelial tight junction permeability. *The Journal of Immunology, 178*(7), 4641–4649. https://doi.org/10.4049/jimmunol.178.7.4641

Angelin, J., & Kavitha, M. (2020). Exopolysaccharides from probiotic bacteria and their health potential. *International Journal of Biological Macromolecules, 162*, 853–865. https://doi.org/10.1016/j.ijbiomac.2020.06.190

Bazaka, K., Crawford, R. J., Nazarenko, E. L., & Ivanova, E. P. (2011). Bacterial extracellular polysaccharides. In D. Linke, & A. Goldman (Eds.), *Vol. 715. Bacterial adhesion* (pp. 213–226). Netherlands: Springer. https://doi.org/10.1007/978-94-007-0940-9_13.

Bochkov, A. Y., & Toukach, P. V. (2021). CSDB/SNFG structure editor: An online glycan builder with 2D and 3D structure visualization. *Journal of Chemical Information and Modeling, 61*(10), 4940–4948. https://doi.org/10.1021/acs.jcim.1c00917

Bravo, B., Correia, P., Gonçalves Junior, J. E., Sant'Anna, B., & Kerob, D. (2022). Benefits of topical hyaluronic acid for skin quality and signs of skin aging: From literature review to clinical evidence. *Dermatologic Therapy, 35*(12). https://doi.org/10.1111/dth.15903

Cao, Y.-Y., Ji, Y.-H., Liao, A.-M., Huang, J.-H., Thakur, K., Li, X.-L., Hu, F., Zhang, J.-G., & Wei, Z.-J. (2020). Effects of sulfated, phosphorylated and carboxymethylated modifications on the antioxidant activities in-vitro of polysaccharides sequentially extracted from Amana edulis. *International Journal of Biological Macromolecules, 146*, 887–896. https://doi.org/10.1016/j.ijbiomac.2019.09.211

Capurso, L. (2019). Thirty years of Lactobacillus rhamnosus GG: A review. *Journal of Clinical Gastroenterology, 53*(Supplement 1), S1–S41. https://doi.org/10.1097/MCG.0000000000001170

Carillo, S., Silipo, A., Perino, V., Lanzetta, R., Parrilli, M., & Molinaro, A. (2009). The structure of the O-specific polysaccharide from the lipopolysaccharide of Burkholderia anthina. *Carbohydrate Research, 344*(13), 1697–1700. https://doi.org/10.1016/j.carres.2009.05.013

Ciucanu, I., & Kerek, F. (1984). A simple and rapid method for the permethylation of carbohydrates. *Carbohydrate Research, 131*(2), 209–217. https://doi.org/10.1016/0008-6215(84)85242-8

DuBois, M., Gilles, K. A., Hamilton, J. K., Rebers, P. A., & Smith, F. (1956). Colorimetric method for determination of sugars and related substances. *Analytical Chemistry, 28*(3), 350–356. https://doi.org/10.1021/ac60111a017

Edgar, R. J., Van Hensbergen, V. P., Ruda, A., Turner, A. G., Deng, P., Le Breton, Y., … Korotkova, N. (2019). Discovery of glycerol phosphate modification on streptococcal rhamnose polysaccharides. *Nature Chemical Biology, 15*(5), 463–471. https://doi.org/10.1038/s41589-019-0251-4

Gorin, P. A. J., & Mazurek, M. (1975). Further studies on the assignment of signals in ^{13}C magnetic resonance spectra of aldoses and derived methyl glycosides. *Canadian Journal of Chemistry, 53*(8), 1212–1223. https://doi.org/10.1139/v75-168

Górska, S., Hermanova, P., Ciekot, J., Schwarzer, M., Srutkova, D., Brzozowska, E., Kozakova, H., & Gamian, A. (2016). Chemical characterization and immunomodulatory properties of polysaccharides isolated from probiotic *Lactobacillus casei* LOCK 0919. *Glycobiology, 26*(9), 1014–1024. https://doi.org/10.1093/glycob/cww047

Górska, S., Schwarzer, M., Jachymek, W., Srutkova, D., Brzozowska, E., Kozakova, H., & Gamian, A. (2014). Distinct immunomodulation of bone marrow-derived dendritic cell responses to Lactobacillus plantarum WCFS1 by two different polysaccharides isolated from Lactobacillus rhamnosus LOCK 0900. *Applied and Environmental Microbiology, 80*(20), 6506–6516. https://doi.org/10.1128/AEM.02104-14

Hu, Q., Lu, Y., & Luo, Y. (2021). Recent advances in dextran-based drug delivery systems: From fabrication strategies to applications. *Carbohydrate Polymers, 264*, Article 117999. https://doi.org/10.1016/j.carbpol.2021.117999

Khan, R., Shah, M. D., Shah, L., Lee, P.-C., & Khan, I. (2022). Bacterial polysaccharides—A big source for prebiotics and therapeutics. *Frontiers in Nutrition, 9*, 1031935. https://doi.org/10.3389/fnut.2022.1031935

Kołodziejska, K., Perepelov, A. V., Zabłotni, A., Drzewiecka, D., Senchenkova, S. N., Zych, K., … Sidorczyk, Z. (2006). Structure of the glycerol phosphate-containing O-polysaccharides and serological studies of the lipopolysaccharides of *Proteus mirabilis* CCUG 10704 (OE) and *Proteus vulgaris* TG 103 classified into a new *Proteus* serogroup, O54. *FEMS Immunology & Medical Microbiology, 47*(2), 267–274. https://doi.org/10.1111/j.1574-695X.2006.00084.x

Laffargue, T., Moulis, C., & Remaud-Siméon, M. (2023). Phosphorylated polysaccharides: Applications, natural abundance, and new-to-nature structures generated by chemical and enzymatic functionalisation. *Biotechnology Advances, 65*, Article 108140. https://doi.org/10.1016/j.biotechadv.2023.108140

Laws, A., Gu, Y., & Marshall, V. (2001). Biosynthesis, characterisation, and design of bacterial exopolysaccharides from lactic acid bacteria. *Biotechnology Advances, 19*(8), 597–625. https://doi.org/10.1016/S0734-9750(01)00084-2

Lee, W., Tonelli, M., & Markley, J. L. (2015). NMRFAM-SPARKY: Enhanced software for biomolecular NMR spectroscopy. *Bioinformatics, 31*(8), 1325–1327. https://doi.org/10.1093/bioinformatics/btu830

Lipkind, G. M., Shashkov, A. S., Knirel, Y. A., Vinogradov, E. V., & Kochetkov, N. K. (1988). A computer-assisted structural analysis of regular polysaccharides on the basis of 13C-n.m.r. Data. *Carbohydrate Research, 175*(1), 59–75. https://doi.org/10.1016/0008-6215(88)80156-3

Liu, T., Ren, Q., Wang, S., Gao, J., Shen, C., Zhang, S., Wang, Y., & Guan, F. (2023). Chemical modification of polysaccharides: a review of synthetic approaches, biological activity and the structure–activity relationship. *Molecules, 28*(16), 6073. https://doi.org/10.3390/molecules28166073

Makino, S., Ikegami, S., Kano, H., Sashihara, T., Sugano, H., Horiuchi, H., … Oda, M. (2006). Immunomodulatory effects of polysaccharides produced by Lactobacillus delbrueckii ssp. Bulgaricus OLL1073R-1. *Journal of Dairy Science, 89*(8), 2873–2881. https://doi.org/10.3168/jds.S0022-0302(06)72560-7

Masuda, Y., Matsumoto, A., Toida, T., Oikawa, T., Ito, K., & Nanba, H. (2009). Characterization and antitumor effect of a novel polysaccharide from Grifola frondosa. *Journal of Agricultural and Food Chemistry, 57*(21), 10143–10149. https://doi.org/10.1021/jf9021338

Mattos, K. A., Jones, C., Heise, N., Previato, J. O., & Mendonça-Previato, L. (2001). Structure of an acidic exopolysaccharide produced by the diazotrophic endophytic bacterium *Burkholderia brasiliensis*. *European Journal of Biochemistry, 268*(11), 3174–3179. https://doi.org/10.1046/j.1432-1327.2001.02196.x

Nagaoka, M., Hashimoto, S., Shibata, H., Kimura, I., Kimura, K., Sawada, H., & Yokokura, T. (1996). Structure of a galactan from cell walls of Bifidobacterium catenulatum YIT4016. *Carbohydrate Research, 281*(2), 285–291. https://doi.org/10.1016/0008-6215(95)00354-1

Nishimura-Uemura, J., Kitazawa, H., Kawai, Y., Itoh, T., Oda, M., & Saito, T. (2003). Functional alteration of murine macrophages stimulated with extracellular polysaccharides from Lactobacillus delbrueckii ssp. Bulgaricus OLL1073R-1. *Food Microbiology, 20*(3), 267–273. https://doi.org/10.1016/S0740-0020(02)00177-6

Pacyga-Prus, K., Jakubczyk, D., Sandström, C., Šrůtková, D., Pyclik, M. J., Leszczyńska, K., … Górska, S. (2023). Polysaccharide BAP1 of Bifidobacterium adolescentis CCDM 368 is a biologically active molecule with immunomodulatory properties. *Carbohydrate Polymers, 315*, Article 120980. https://doi.org/10.1016/j.carbpol.2023.120980

Prateeksha, Sharma, V. K., Liu, X., Oyarzún, D. A., Abdel-Azeem, A. M., Atanasov, A. G., … Singh, B. N. (2022). Microbial polysaccharides: An emerging family of natural biomaterials for cancer therapy and diagnostics. *Seminars in Cancer Biology, 86*, 706–731. https://doi.org/10.1016/j.semcancer.2021.05.021

Pyclik, M., Srutkova, D., Schwarzer, M., & Górska, S. (2020). Bifidobacteria cell wall-derived exo-polysaccharides, lipoteichoic acids, peptidoglycans, polar lipids and proteins – Their chemical structure and biological attributes. *International Journal of Biological Macromolecules, 147*, 333–349. https://doi.org/10.1016/j.ijbiomac.2019.12.227

Pyclik, M. J., Srutkova, D., Razim, A., Hermanova, P., Svabova, T., Pacyga, K., … Górska, S. (2021). Viability status-dependent effect of Bifidobacterium longum ssp. Longum CCM 7952 on prevention of allergic inflammation in mouse model. *Frontiers in Immunology, 12*, 2800. https://doi.org/10.3389/fimmu.2021.707728

Rafique, N., Jan, S. Y., Dar, A. H., Dash, K. K., Sarkar, A., Shams, R., … Hussain, S. Z. (2023). Promising bioactivities of postbiotics: A comprehensive review. *Journal of Agriculture and Food Research, 14*, Article 100708. https://doi.org/10.1016/j.jafr.2023.100708

Salazar, N., Prieto, A., Leal, J. A., Mayo, B., Bada-Gancedo, J. C., De Los Reyes-Gavilán, C. G., & Ruas-Madiedo, P. (2009). Production of exopolysaccharides by Lactobacillus and Bifidobacterium strains of human origin, and metabolic activity of the producing bacteria in milk. *Journal of Dairy Science, 92*(9), 4158–4168. https://doi.org/10.3168/jds.2009-2126

Salminen, S., Collado, M. C., Endo, A., Hill, C., Lebeer, S., Quigley, E. M. M., … Vinderola, G. (2021). The international scientific Association of Probiotics and Prebiotics (ISAPP) consensus statement on the definition and scope of postbiotics. *Nature Reviews Gastroenterology & Hepatology, 18*(9), 649–667. https://doi.org/10.1038/s41575-021-00440-6

Sato, T., Nishimura-Uemura, J., Shimosato, T., Kawai, Y., Kitazawa, H., & Saito, T. (2004). Dextran from Leuconostoc mesenteroides augments Immunostimulatory effects by the introduction of phosphate groups. *Journal of Food Protection, 67*(8), 1719–1724. https://doi.org/10.4315/0362-028X-67.8.1719

Sawardeker, J. S., Sloneker, J. H., & Jeanes, A. (1965). Quantitative determination of monosaccharides as their Alditol acetates by gas liquid chromatography. *Analytical Chemistry, 37*(12), 1602–1604. https://doi.org/10.1021/ac60231a048

Schiavi, E., Plattner, S., Rodriguez-Perez, N., Barcik, W., Frei, R., Ferstl, R., … O'Mahony, L. (2018). Exopolysaccharide from *Bifidobacterium longum* subsp. *Longum* 35624™ modulates murine allergic airway responses. *Beneficial Microbes, 9*(5), 761–773. https://doi.org/10.3920/BM2017.0180

Senchenkova, S. N., Shashkov, A. S., Laux, P., Knirel, Y. A., & Rudolph, K. (1999). The O-chain polysaccharide of the lipopolysaccharide of Xanthomonascampestris pv. Begoniae GSPB 525 is a partially l-xylosylated l-rhamnan. *Carbohydrate Research, 319*(1–4), 148–153. https://doi.org/10.1016/S0008-6215(99)00125-1

Shashkov, A. S., Lipkind, G. M., Knirel, Y. A., & Kochetkov, N. K. (1988a). Stereochemical factors determining the effects of glycosylation on the ^{13}C chemical shifts in carbohydrates. *Magnetic Resonance in Chemistry, 26*(9), 735–747. https://doi.org/10.1002/mrc.1260260904

Shashkov, A. S., Lipkind, G. M., Knirel, Y. A., & Kochetkov, N. K. (1988b). Stereochemical factors determining the effects of glycosylation on the13C chemical shifts in carbohydrates. *Magnetic Resonance in Chemistry, 26*(9), 735–747. https://doi.org/10.1002/mrc.1260260904

Speciale, I., Verma, R., Di Lorenzo, F., Molinaro, A., Im, S.-H., & De Castro, C. (2019). Bifidobacterium bifidum presents on the cell surface a complex mixture of glucans and galactans with different immunological properties. *Carbohydrate Polymers, 218*, 269–278. https://doi.org/10.1016/j.carbpol.2019.05.006

Srutkova, D., Kozakova, H., Novotna, T., Gorska, S., Hermanova, P. P., Hudcovic, T., … Schwarzer, M. (2023). Exopolysaccharide from *Lacticaseibacillus rhamnosus* induces IgA production in airways and alleviates allergic airway inflammation in mouse model. *European Journal of Immunology, 53*(7), 2250135. https://doi.org/10.1002/eji.202250135

Srutkova, D., Schwarzer, M., Hudcovic, T., Zakostelska, Z., Drab, V., Spanova, A., … Schabussova, I. (2015). Bifidobacterium longum CCM 7952 promotes epithelial barrier function and prevents acute DSS-induced colitis in strictly strain-specific manner. *PLoS One, 10*(7), Article e0134050. https://doi.org/10.1371/journal.pone.0134050

Sunil, Y., Ramadori, G., & Raddatz, D. (2010). Influence of NFκB inhibitors on IL-1β-induced chemokine CXCL8 and −10 expression levels in intestinal epithelial cell lines: Glucocorticoid ineffectiveness and paradoxical effect of PDTC. *International Journal of Colorectal Disease, 25*(3), 323–333. https://doi.org/10.1007/s00384-009-0847-3

Toukach, P. V. (2011). Bacterial carbohydrate structure database 3: Principles and realization. *Journal of Chemical Information and Modeling, 51*(1), 159–170. https://doi.org/10.1021/ci100150d

Verma, R., Lee, C., Jeun, E.-J., Yi, J., Kim, K. S., Ghosh, A., … Im, S.-H. (2018). Cell surface polysaccharides of *Bifidobacterium bifidum* induce the generation of Foxp3 $^{+}$

regulatory T cells. *Science Immunology, 3*(28), Article eaat6975. https://doi.org/10.1126/sciimmunol.aat6975

Vichai, V., & Kirtikara, K. (2006). Sulforhodamine B colorimetric assay for cytotoxicity screening. *Nature Protocols, 1*(3), 1112–1116. https://doi.org/10.1038/nprot.2006.179

Vinogradov, E., Korenevsky, A., & Beveridge, T. J. (2003). The structure of the O-specific polysaccharide chain of the Shewanella algae BrY lipopolysaccharide. *Carbohydrate Research, 338*(4), 385–388. https://doi.org/10.1016/S0008-6215(02)00469-X

You, X., Li, Z., Ma, K., Zhang, C., Chen, X., Wang, G., Yang, L., Dong, M., Rui, X., Zhang, Q., & Li, W. (2020). Structural characterization and immunomodulatory activity of an exopolysaccharide produced by Lactobacillus helveticus LZ-R-5. *Carbohydrate Polymers, 235*, Article 115977. https://doi.org/10.1016/j.carbpol.2020.115977

Zeidan, A. A., Poulsen, V. K., Janzen, T., Buldo, P., Derkx, P. M. F., Øregaard, G., & Neves, A. R. (2017). Polysaccharide production by lactic acid bacteria: From genes to industrial applications. *FEMS Microbiology Reviews, 41*(Supp_1), S168–S200. https://doi.org/10.1093/femsre/fux017

Zhou, Y., Cui, Y., & Qu, X. (2019). Exopolysaccharides of lactic acid bacteria: Structure, bioactivity and associations: A review. *Carbohydrate Polymers, 207*, 317–332. https://doi.org/10.1016/j.carbpol.2018.11.093